

# A Critical Review for Proper Use of Water/Oil/Gas Transfer Functions in Dual-Porosity Naturally Fractured Reservoirs: Part II

M. Al-Kobaisi, SPE, H. Kazemi, SPE, B. Ramirez,\* SPE, and E. Ozkan, SPE, Colorado School of Mines; and S. Atan, SPE, Marathon Oil Corporation

## Summary

This paper continues the work presented in Ramirez et al. (2009). In Part I, we discussed the viability of the use of simple transfer functions to accurately account for fluid exchange as the result of capillary, gravity, and diffusion mass transfer for immiscible flow between fracture and matrix in dual-porosity numerical models. Here, we show additional information on several relevant topics, which include (1) flow of a low-concentration water-soluble surfactant in the fracture and the extent to which the surfactant is transported into the matrix; (2) an adjustment to the transfer function to account for the early slow mass transfer into the matrix before the invading fluid establishes full connectivity with the matrix; and (3) an analytical approximation to the differential equation of mass transfer from the fracture to the matrix and a method of solution to predict oil-drainage performance.

Numerical experiments were performed involving single-porosity, fine-grid simulation of immiscible oil recovery from a typical matrix block by water, gas, or surfactant-augmented water in an adjacent fracture. Results emphasize the viability of the transfer-function formulations and their accuracy in quantifying the interaction of capillary and gravity forces to produce oil depending on the wettability of the matrix. For miscible flow, the fracture/matrix mass transfer is less complicated because the interfacial tension (IFT) between solvent and oil is zero; nevertheless, the gravity contrast between solvent in the fracture and oil in the matrix creates convective mass transfer and drainage of the oil.

## Introduction

Characterization and quantification of fractures in naturally fractured reservoirs is a very difficult task; nonetheless, when natural fractures contribute significantly to fluid movement and hydrocarbon drainage in the reservoir, a dual-porosity approach is adopted to quantify reservoir performance. The dual-porosity concept can be perceived and quantified in several ways, as shown in Fig. 1.

The dual-porosity concept was conceived on the premise that a very highly conductive fracture medium was formed as an interconnected network of secondary porosity within a pre-existing porous rock of primary porosity. A third medium of lower-conductivity fractures (i.e., microfractures) can be added to the flow system in some important applications. Regardless of the formulation, the flow in the high-conductivity fracture network takes place at high velocities from one grid cell to another irrespective of the flowing phase. In two- or three-phase flow, there is usually a local exchange of fluids between the fractures and the adjacent matrix at comparatively low velocities. Contrast in fluid velocities in the two flow systems is a very important issue in naturally fractured reservoirs because, in multiphase flow, typically water or gas can move rapidly in the fractures and surround the matrix blocks partially or totally. Once a matrix block is sur-

rounded partially or totally by a particular fluid, then transfer of fluid phases and components takes place between the fracture and matrix. Deciphering the recovery mechanisms and describing the pertinent equations of mass transfer constitute the heart of this paper—both Part I (Ramirez et al. 2009) and Part II. Similar issues extend to any variants of the dual-porosity concept, such as the triple-porosity, irrespective of the idealization concept.

## Literature Review

The heart of the dual-porosity multiphase-flow modeling is the transfer function that accounts for the transfer of fluids between the fracture and the matrix (Barenblatt et al. 1960; Warren and Root 1963; Kazemi et al. 1976; Litvak 1985; Sonier et al. 1988; Gilman and Kazemi 1988; Balogun et al. 2007).

The foundations of the current models were laid by Barenblatt et al. (1960) and Warren and Root (1963). These authors dealt with the mathematical formulation of single-phase flow in dual-porosity systems. The material-balance equation that described the transfer function  $\tau$ , defined as the flow rate per unit of rock volume, had the general form shown here:

$$\tau = \sigma \frac{k}{\mu} (p_m - p_f), \dots \dots \dots (1)$$

where  $\sigma$  is the shape factor;  $k$  is matrix permeability;  $\mu$  is fluid viscosity; and  $(p_m - p_f)$  is pressure difference between the matrix and fracture. Warren and Root (1963) provided an analytical solution for radial flow for well-testing purposes and idealized a fractured reservoir as a set of stacked sugar cubes. Kazemi et al. (1976) extended the Warren and Root (1963) model to water/oil flow and developed a numerical algorithm to solve the fracture-flow equations while accounting for matrix/fracture fluid transfer using a multiphase transfer function.

Hydrocarbon reservoirs produce fluids under a combination of mechanisms including capillarity, gravity drainage, viscous displacement, pore compaction, and fluid expansion. Depending on the flowing phases present, capillary and gravity forces are generally dominant in fractured reservoirs. These forces can work in tandem or can oppose each other (Gilman 2003).

Sonier et al. (1988) and Litvak (1985) provided a dynamic approach to improve the modeling of the interaction of gravity and capillary forces in the matrix/fracture system without fine gridding. Gilman (1986), however, used a fine-grid approach to develop a more accurate method to account for gravity forces better.

Another issue is the viscous displacement in the matrix blocks of the dual-porosity models. Gilman and Kazemi (1988) presented a formulation to account for this effect. Viscous displacement is much more significant in single-porosity systems.

Results from imbibition experiments (Mattax and Kyte 1962), centrifuge experiments (Kyte 1970), physical models (Kleppe and Morse 1974), fractured corefloods (Kazemi and Merrill 1979), stacked cores (Horie et al. 1990), and newer imbibition experiments (Morrow et al. 1995) provided the foundation for scaling laboratory results to field conditions.

Fung (1991) and Uleberg and Kleppe (1996) dealt with finer details of simulating gravity drainage in dual-porosity reservoirs including the effect of oil reinfiltration from one block to a block underneath, which could lead to lower oil recovery from the fractures under specific conditions.

\*Now with Marathon Oil Corporation.

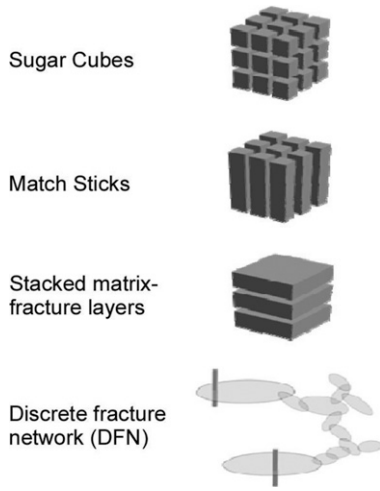


**Fig. 1—Four common idealizations of naturally fractured reservoir models.**

The magnitude of capillary pressure in the fracture is difficult to assess. However, if one assumes that there is some capillary continuity between matrix blocks across the fractures, then a match-stick dual-permeability model can be used as opposed to the dual-porosity model (Fung and Collins 1991).

Additional light was shed on the mechanism of oil production from naturally fractured reservoirs by gravity drainage, capillary interaction, and IFT reduction; this was reported by Saidi (1983), Kazemi and Gilman (1993), Al-Kandari (2002), and Liu et al. (2006). All these papers tried to explain the mechanisms of oil production from matrix to fracture.

Research results are also available from laboratory investigations and related numerical simulations of fractured systems on a single matrix block (Blair 1964; Ifly et al. 1972; Kleppe and Morse 1974). Yamamoto et al. (1971) developed the earliest compositional model for studying recovery mechanisms from single matrix blocks surrounded by different fluids.

In Part I of the paper, we presented a thorough physical perspective on the evolution of transfer functions as simple and effective means to calculate the transfer of fluids and components between fracture and matrix. Similarly, we explained the evolution of the shape factor, which is a geometric component of the surface area, the volume, and the distance from the matrix center to the fracture.

### Transfer Function–Component Convection and Diffusion in Dual-Porosity Water/Oil Systems

We have shown in Part I of the paper that the transfer-function equation for the dual-porosity, water/oil system takes the following form:

$$\tau_w = \left\{ \begin{array}{l} \sigma k_m \left( \frac{\lambda_{wf/m} \lambda_{om/f}}{\lambda_T} \right) \left[ \begin{array}{l} (p_{cwom} - p_{cwof}) \\ + \left( \frac{\sigma_z}{\sigma} \right) (\gamma_w - \gamma_o) (h_{wf} - h_{wm}) \end{array} \right] \\ + \left( \frac{\lambda_{wf/m}}{\lambda_T} \right) \left[ \begin{array}{l} \phi_m c_{Tm} \frac{\partial p_{om}}{\partial t} \\ - \phi_m S_{wm} (c_{wm} + c_{\phi m}) \frac{\partial p_{cwom}}{\partial t} \end{array} \right] \end{array} \right\} \dots \dots \dots (2)$$

and the water-saturation equation for the dual-porosity flow was given by

$$\begin{array}{l} - \left[ \begin{array}{l} (\nabla \cdot f_{wf} \vec{v}_{Tf} + \vec{G}_{wf} + \vec{C}_{wf}) \\ - \tau_w \end{array} \right] \\ = \left[ \begin{array}{l} \phi_f \frac{\partial S_{wf}}{\partial t} \\ + \phi_f S_{wf} (c_{wf} + c_{\phi f}) \frac{\partial p_{wf}}{\partial t} \end{array} \right] \dots \dots \dots (3) \end{array}$$

In Eqs. 2 and 3,

$$\tau_w = \phi_m \frac{\partial S_{wm}}{\partial t} + \phi_m S_{wm} (c_{wm} + c_{\phi m}) \left( \frac{\partial p_{om}}{\partial t} - \frac{\partial p_{cwom}}{\partial t} \right), \dots \dots \dots (4)$$

$$\vec{G}_{wf} = f_{wf} \lambda_{of} \bar{k}_f (\gamma_w - \gamma_o) \nabla D_f, \dots \dots \dots (5)$$

$$\vec{C}_{wf} = f_{wf} \lambda_{of} \bar{k}_f \nabla p_{cwof}, \dots \dots \dots (6)$$

$$\lambda_t = \lambda_{wf/m} + \lambda_{om/f}, \dots \dots \dots (7)$$

$$h_{wf} = \left[ \frac{S_{wf} - S_{wrf}}{1 - S_{orwf} - S_{wrf}} \right] L_z, \dots \dots \dots (8)$$

and

$$h_{wm} = \left[ \frac{S_{wm} - S_{wrm}}{1 - S_{orwm} - S_{wrm}} \right] L_z. \dots \dots \dots (9)$$

Now, let us assume that the water phase contains a diffusive low-concentration tracer or surfactant. To account for the convection and diffusion of tracer in and out of a matrix block, the transfer function for water containing tracer takes the following form:

$$\tau_w C_{sf/m} = \left\{ \begin{array}{l} \sigma k_m \left( \frac{\lambda_{wf/m} \lambda_{om/f}}{\lambda_T} \right) \left[ \begin{array}{l} (p_{cwom} - p_{cwof}) \\ + \left( \frac{\sigma_z}{\sigma} \right) (\gamma_w - \gamma_o) (h_{wf} - h_{wm}) \end{array} \right] \\ + \left( \frac{\lambda_{wf/m}}{\lambda_T} \right) \left[ \begin{array}{l} \phi_m c_{Tm} \frac{\partial p_{om}}{\partial t} \\ - \phi_m S_{wm} (c_{wm} + c_{\phi m}) \frac{\partial p_{cwom}}{\partial t} \end{array} \right] \\ + \sigma \left[ \frac{D}{\tau} \phi S_w \right]_m (C_{sf} - C_{sm}) \end{array} \right\} C_{sf/m} \dots \dots \dots (10)$$

Similarly, the water-flow equations for fracture and matrix, Eqs. 11 and 12, respectively, take the following form:

$$\begin{array}{l} \left\{ \begin{array}{l} - \left[ \begin{array}{l} (\nabla \cdot f_{wf} \vec{v}_{Tf} + \nabla \cdot \vec{G}_{wf} + \nabla \cdot \vec{C}_{wf}) C_{sf} \\ - \nabla \cdot \left( \frac{D}{\tau} \phi S_w \right)_f \nabla C_{sf} \end{array} \right] \\ - \tau_w C_{sf/m} \end{array} \right\} \\ = \left[ \begin{array}{l} \phi \frac{\partial (S_{wf} C_{sf})}{\partial t} \\ + \phi (S_{wf} C_{sf}) (c_{wf} + c_{\phi f}) \frac{\partial p_{wf}}{\partial t} \\ + (1 - \phi_f) (1 \times 10^6 SG_{solid}) \frac{\partial a_f}{\partial t} \end{array} \right] \dots \dots \dots (11) \end{array}$$

and

$$\tau_w C_{sf/m} = \left[ \begin{array}{l} \phi_m \frac{\partial (S_{wm} C_{sf/m})}{\partial t} \\ + \phi_m (S_{wm} C_{sf/m}) (c_{wm} + c_{\phi m}) \left( \frac{\partial p_{om}}{\partial t} - \frac{\partial p_{cwom}}{\partial t} \right) \\ + (1 - \phi_m) (1 \times 10^6 SG_{solid}) \frac{\partial a_m}{\partial t} \end{array} \right], \dots \dots \dots (12)$$

where,

$$a_m (C_{sf/m}) = \left( \frac{b_{f/m} C_{sf/m}}{1 + b_{f/m} C_{sf/m}} \right) a_{m \max} \dots \dots \dots (13)$$

### Analysis of Results

**Tracer/Surfactant Transport Simulation.** A 10×10×10 ft matrix block containing water and oil was flooded with water containing an adsorbing tracer to simulate the transport of a low-concentration surfactant. Water-soluble tracer solution was injected horizontally at a constant pressure gradient of 0.01 psi/ft in one end of the vertical fracture. A Langmuir adsorption iso-

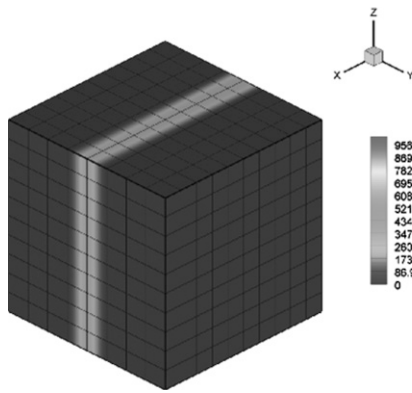


**Fig. 2—Surfactant penetration into the matrix from fracture flow.**

therm with a maximum adsorption of 0.80 mg/g of rock was chosen. A molecular-diffusion coefficient  $0.001 \text{ ft}^2/\text{D}$  was used. The fine-grid simulation is shown in **Figs. 2 and 3**. The results indicate clearly that tracer or surfactant could potentially penetrate only a short distance into the matrix. This conclusion is consistent with field observations and the response from the injection of wettability-altering surfactants in the 1990s in a naturally fractured carbonate reservoir in Permian Basin, Texas. In fact, early tracer breakthrough and high tracer peaks from wells in this area of the field [shown graphically in Kazemi et al. (2005) and Shinta and Kazemi (1993)] support this conclusion. Also, the recent paper by Stoll et al. (2008) arrives at a similar conclusion, stating that: “In any diffusion process, the time scale is linked to the square of the length scale of the medium. Therefore, it would take up to 1,000 times longer (an equivalent of 200 years) before the same recovery is obtained from a meter-scale matrix block as is obtained from a centimeter-scale plug in a laboratory in 100 days. Consequently, unless a significantly faster transport mechanism for the wettability modifier is identified, or unless viscous forces or buoyancy enable forced imbibition, the chemical wettability modification of fractured oil-wet carbonate rock does not provide an economically interesting opportunity.”

**Gas/Oil Simulation.** In Part I (Ramirez et al. 2009), a numerical model to study gas-invoked oil drainage from a matrix block was constructed using a multicomponent-fluid system. We are repeating part of the results here because the numerical oil-recovery results are typically somewhat more optimistic at early times than in laboratory experiments. In other words, in laboratory experiments, the early-time oil drainage is slower than in numerical models (Morrow et al. 1995). Here, we will show how we can adjust the response of the transfer functions to account for the laboratory observations. Eclipse 300 (Schlumberger Oilfield Services; 2005A; Houston) was used to generate oil-drainage-vs.-time plots. The oil recovery from the matrix for three levels of

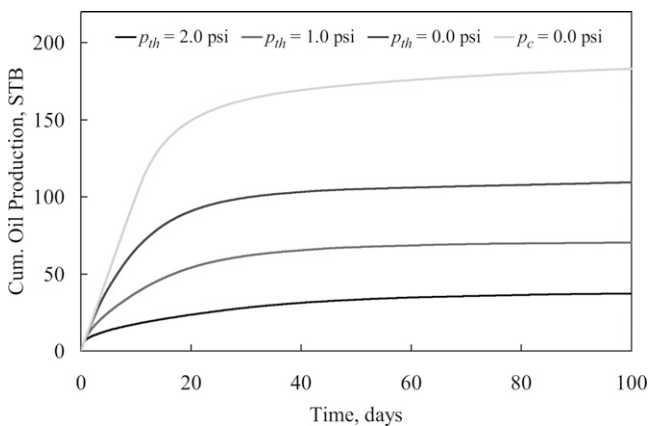


**Fig. 4—Fine-grid simulated oil recovery as a function of capillary holdup pressure.**

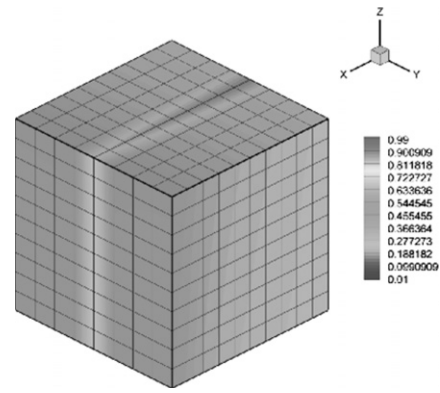


**Fig. 3—Water-saturation profile.**

gas-oil capillary holdup pressure (or the capillary threshold) is shown in **Fig. 4**. This figure clearly shows the enormous sensitivity of oil drainage to the capillary holdup pressure. The molecular-diffusion effect was rather small, as was shown in Part I of the paper. **Fig. 5** shows the 3D gas/oil-saturation distribution for the three levels of gas/oil capillary holdup pressure.

Interestingly enough, as an added dimension to the utility of the transfer function, we used the following simple form of the gas/oil-transfer function (incompressible, noncompositional Buckley-Leverett approach) and the associated material-balance

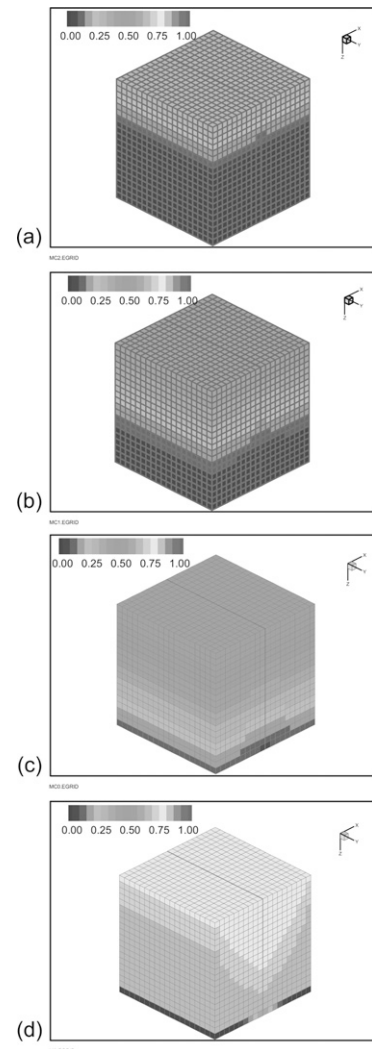


**Fig. 5—Fine-grid simulated gas-saturation profile with different capillary holdup pressures (from top to bottom,  $p_{th} = 2$  psia,  $p_{th} = 1$  psia,  $p_{th} = 0$ , and  $p_c = 0$ ).**

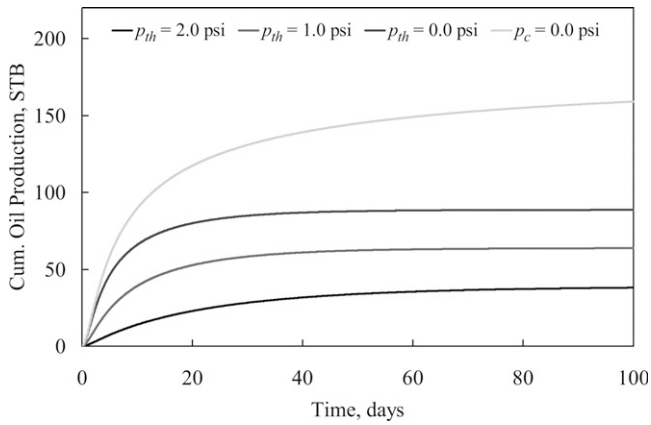


Fig. 6—Transfer-function oil recoveries.

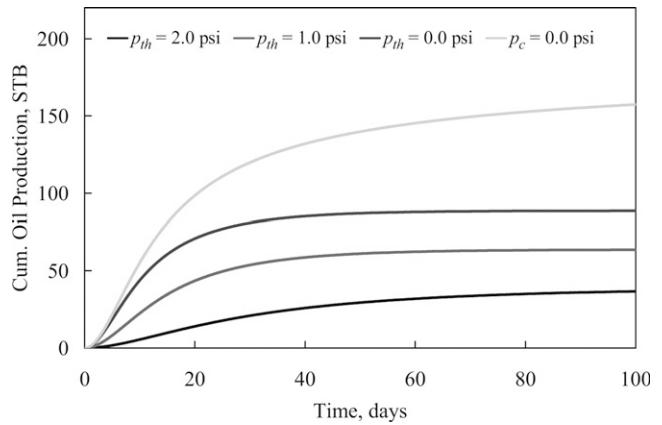


Fig. 7—Transfer-function oil recoveries with early-time delay effects.

equation to calculate oil recovery from the matrix to see how the results compare with the numerical results.

$$-\sigma k_m \frac{\lambda_{gf}^n / m \lambda_{o,m}^n / f}{\lambda_T^n} \left[ \begin{array}{l} -(p_{cgom}^n - p_{cgo}^n) \\ + \left(\frac{\sigma_z}{\sigma}\right) (\gamma_o^n - \gamma_g^n) (h_{gf}^n - h_{gm}^n) \end{array} \right], \dots (14)$$

$$= \phi_m \frac{\partial S_{om}}{\partial t} \approx \phi_m \frac{S_o^{n+1} - S_o^n}{\Delta t}$$

where

$$h_{gf} = \left( \frac{S_{gf}}{1 - S_{wrf} - S_{orf}} \right) L_z \dots (15)$$

and

$$h_{gm} = \left( \frac{S_{gm}}{1 - S_{wrm} - S_{orm}} \right) L_z \dots (16)$$

The results of using Eq. 14 are shown in Fig. 6 and compare extremely well with the simulation results shown in Fig. 4, given that the transfer function used was not the compositional one presented in Part I. In the compositional model (Eclipse), gas entering the matrix blocks mixes with the entire hydrocarbon system, including the residual oil; thus, higher recovery is often expected, which is consistent with our results. Another issue is that in the simulation runs, in order to create a physically realistic boundary condition in the fracture, we injected gas on top and produced from the bottom. If the gas-injection rate is of high velocity, it creates a potential gradient in the fracture, which makes gas appear as if it is lighter in comparison to static conditions. Similarly, if we inject water at the bottom of the fracture to move upward toward the top, because of the viscous resistance to flow, it creates potential gradients, which makes water appear as if it is heavier than in the static conditions. Both of these effects can be calculated and lead to an effective gas gradient and an effective water gradient (Appendix).

Back to the laboratory observation issue, an adjustment was made to the gas/oil transfer function to account for the early slow mass transfer into matrix before the invading gas establishes full connectivity with the matrix. The result of our computational adjustment is shown in Fig. 7. The adjustment involves a premultiplier to the transfer function, either as a time or a saturation function shown here, respectively:

$$\{1 - \exp[-(\zeta_t t + 0.0001)]\}, \dots (17)$$

$$\{1 - \exp[-(\zeta_s S_g + 0.0001)]\}. \dots (18)$$

The time premultiplier  $\zeta_t$  for our example is 0.1, and the saturation premultiplier  $\zeta_s$  is 100. Similar time or saturation premultipliers can be used to conform to physical evidence.

Here is another interesting observation. By comparing the transfer functions of this paper with the 1D gas/oil gravity-drainage theory (Alkandari 2002) and with the numerical results of this work, we infer that when flow is dominated by gravity drainage, then  $\sigma_z/\sigma$  should be set equal to one. Furthermore, the lefthand side of Eq. 14 can be written as a function of  $S_o$ , say  $f(S_o)$ . Then, Eq. 14 becomes

$$-\frac{\sigma k_m \lambda_{om} (\gamma_o - \gamma_g) (L_z)}{\phi_m} [f(S_o)] = \frac{dS_o}{dt}, \dots (19)$$

or

$$\frac{dS_o}{f(S_o)} = -\frac{\sigma k_m \lambda_{om} (\gamma_o - \gamma_g) (L_z)}{\phi_m} dt. \dots (20)$$

Integration of Eq. 20 from the initial oil saturation to the saturation at which the capillary/gravity component of the transfer function becomes zero, gives an oil-recovery curve similar to the ones shown in Fig. 6. In fact, if one approximates  $f(S_o)$  by a low-order polynomial of order two or three, then  $1/f(S_o)$  can be expanded by partial fractions, where the first term involving  $1/S_o$  leads to an exponential term. This term is generally the major contributor to the shape of the recovery curve  $R = R_\infty(1 - e^{-nt})$ .

For pure gravity drainage, the 1D frontal displacement is given by

$$-\frac{\partial}{\partial z} \left\{ k_m \lambda_o \left[ (\gamma_o - \gamma_g) + \frac{\partial p_{cgom}}{\partial z} \right] \right\} = \phi_m \frac{\partial S_o}{\partial t} \dots (21)$$

In finite-difference form, Eq. 21 can be approximated by

$$-\frac{1}{(L_z/2)^2} \left\{ k_m \lambda_o \left[ -p_{cogm}(S_o) + L_z (\gamma_o - \gamma_g) \right] \right\} = \phi_m \frac{\partial S_o}{\partial t} \dots (22)$$

Eq. 22 is very similar to Eq. 14 and implies that the coefficient  $\sigma_z/\sigma$  is numerically equal to one for gravity-drainage-dominated situations.

## Conclusions

This paper is Part II to Ramirez et al. (2009) on transfer functions for dual-porosity reservoirs. The objective of the paper is to provide supplementary critical information on the proper use of the matrix/fracture transfer functions. Below is a summary of our findings:

- We established that tracer or surfactant could potentially penetrate only a short distance into the matrix; thus, an enhanced-oil-recovery issue.
- We made a simple mathematical adjustment to the transfer function to account for the early slow mass transfer into matrix before the invading fluid establishes full connectivity with the matrix.

- We presented an analytical approximation to the differential equation of the transfer function.
- We established that the coefficient  $\sigma_z/\sigma$  is one for gravity-drainage-dominated situations.

## Nomenclature

$a$	= vertical flow potential gradient, psi/ft
$a_m$	= surfactant adsorption, g of surfactant/g of rock
$a_{m \max}$	= maximum surfactant adsorption, g of surfactant/g of rock
$b_{f/m}$	= Langmuir coefficient in fracture or matrix, ppm <sup>-1</sup>
$c_t$	= total compressibility, psi <sup>-1</sup>
$c_\phi$	= pore compressibility, psi <sup>-1</sup>
$C_s$	= surfactant concentration in water phase, ppm
$\vec{C}_w$	= capillary-force-flow velocity vector, ft/D
$D$	= depth, ft
$f_w$	= fractional flow, fraction
$\vec{G}_w$	= gravity-force flow-velocity vector, ft/D
$h$	= gravity head, ft
$L$	= matrix-block dimension, ft
$k$	= $0.006328 \times$ absolute permeability, md
$k_r$	= relative permeability
$p$	= pressure, psi
$q$	= flow rate, surface ft <sup>3</sup> /day
$R$	= fractional recovery
$S$	= saturation, fraction
$S_{orw}$	= residual-oil saturation to water
$S_{wr}$	= irreducible water saturation
$SG_{\text{solid}}$	= specific gravity of the rock matrix
$t$	= time, days
$\vec{v}$	= Darcy velocity vector, ft/day
$w_f$	= fracture width, ft
$\gamma$	= fluid gravity gradient, psi/ft
$\zeta$	= premultiplier
$\lambda$	= mobility coefficient, cp <sup>-1</sup>
$\mu$	= viscosity, cp
$\rho$	= density, lbm/ft <sup>3</sup>
$\sigma$	= matrix-block shape factor, 1/ft <sup>2</sup>
$\tau$	= matrix/fracture transfer function, 1/days
$\phi$	= porosity, fraction
$\Phi$	= flow potential, psi

## Subscripts

$c$	= component
$f$	= fracture
$g$	= gas
$m$	= matrix
$o$	= oil
$s$	= saturation
$th$	= threshold
$T$	= total
$w$	= water
$x$	= x-direction
$y$	= y-direction
$z$	= z-direction

## Superscripts

$n$	= previous time level
$n+1$	= current time level

## Acknowledgments

This research was conducted at the Marathon Center of Excellence for Reservoir Studies (MCERS) at Colorado School of Mines. We acknowledge the funding by Marathon Oil Corporation, Abu Dhabi National Oil Company, Saudi Aramco, Pemex, and Repsol-YPF.

## References

- Al-Kandari, H.A. 2002. Numerical simulation of gas-oil gravity drainage for centrifuge experiments and scaled reservoir matrix blocks. PhD dissertation, Colorado School of Mines, Golden, Colorado.
- Al-Kandari, H.A., Kazemi, H., and Van Kirk, C.W. 2002. Gas injection enhanced oil recovery in high relief naturally fractured reservoirs. Presented at the Kuwait International Petroleum Conference and Exhibition, Kuwait City, State of Kuwait, 14–16 December.
- Balogun, A., Kazemi, H., Ozkan, E., Al-Kobaisi, A., and Ramirez, B. 2007. Verification and Proper Use of Water/Oil Transfer Function for Dual-Porosity and Dual-Permeability Reservoirs. Paper SPE 104580 presented at the SPE Middle East Oil and Gas Show and Conference, Kingdom of Bahrain, 11–14 March. DOI: 10.2118/104580-MS.
- Barenblatt, G.I., Zheltov, I.P., and Kochina, I.N. 1960. Basic concepts in the theory of seepage of homogeneous liquids in fissured rocks. *J. of Applied Mathematics and Mechanics* **24** (5): 1286–1303. DOI:10.1016/0021-8928(60)90107-6.
- Blair, P.M. 1964. Calculation of Oil Displacement by Countercurrent Water Imbibition. *SPE J.* **4** (3): 195–202; *Trans.*, AIME, **231**. SPE-873-PA. DOI: 10.2118/873-PA.
- Fung, L.S.K. 1991. Simulation of Block-to-Block Processes in Naturally Fractured Reservoirs. *SPE Res Eng* **6** (4): 477–484. SPE-20019-PA. DOI: 10.2118/20019-PA.
- Gilman, J.R. 1986. An Efficient Finite-Difference Method for Simulating Phase Segregation in the Matrix Blocks in Double-Porosity Reservoirs. *SPE Res Eng* **1** (4): 403–413; *Trans.*, AIME, **281**. SPE-12271-PA. DOI: 10.2118/12271-PA.
- Gilman, J.R. 2003. Practical aspects of simulation of naturally fractured reservoirs. Presented at the International Forum on Reservoir Simulation, Buhl, Baden-Baden, Germany, 23–27 June.
- Gilman, J.R. and Kazemi, H. 1988. Improved Calculations for Viscous and Gravity Displacement in Matrix Blocks in Dual-Porosity Simulators. *J. Pet Tech* **40** (1): 60–70; *Trans.*, AIME, **285**. SPE-16010-PA. DOI: 10.2118/16010-PA.
- Horie, T., Firoozabadi, A., and Ishimoto, K. 1990. Laboratory Studies of Capillary Interaction in Fracture/Matrix Systems. *SPE Res Eng* **5** (3): 353–360. SPE-18282-PA. DOI: 10.2118/18282-PA.
- Iffly, R., Rousselet, D.C., and Vermeulen, J.L. 1972. Fundamental Study of Imbibition in Fissured Oil Fields. Paper SPE 4102 presented at the Annual Meeting of the Society of Petroleum Engineers of AIME, San Antonio, Texas, USA, 8–11 October. DOI: 10.2118/4102-MS.
- Kazemi, H. and Gilman, J.R. 1993. Multiphase flow in fractured petroleum reservoirs. In *Flow and Contaminant Transport in Fractured Rock*, ed. J. Bear, C.-F. Tsang, G. de Marsily, 267–323. San Diego, California: Academic Press.
- Kazemi, H. and Merrill, L.S. 1979. Numerical Simulation of Water Imbibition in Fractured Cores. *SPE J.* **19** (3): 175–182. SPE-6895-PA. DOI: 10.2118/6895-PA.
- Kazemi, H., Gilman, J.R. and Elsharkawy, A.M. 1992. Analytical and Numerical Solution of Oil Recovery From Fractured Reservoirs With Empirical Transfer Functions. *SPE Res Eng* **7** (2): 219–227. SPE-19849-PA. DOI: 10.2118/19849-PA.
- Kazemi, H., Merrill, J.R., Porterfield, K.L., and Zeman, P.R. 1976. Numerical Simulation of Water-Oil Flow in Naturally Fractured Reservoirs. *SPE J.* **16** (6): 317–326; *Trans.*, AIME, **261**. SPE-5719-PA. DOI: 10.2118/5719-PA.
- Kleppe, J. and Morse, R.A. 1974. Oil Production From Fractured Reservoirs by Water Displacement. Paper SPE 5084 presented at the Annual Meeting of the Society of Petroleum Engineers of AIME, Houston, 6–9 October. DOI: 10.2118/5084-MS.
- Kyte, J.R. 1970. A Centrifuge Method To Predict Matrix-Block Recovery in Fractured Reservoirs. *SPE J.* **10** (2): 161–170; *Trans.*, AIME, **249**. SPE-2729-PA. DOI: 10.2118/2729-PA.
- Litvak, B.L. 1985. Simulation and characterization of naturally fractured reservoirs. *Proc.*, Reservoir Characterization Technical Conference, Dallas, 561–583.
- Lu, H., Di Donato, G., and Blunt, M.J. 2006. General Transfer Functions for Multi-Phase Flow. Paper SPE 102542 presented at the SPE Annual Technical Conference and Exhibition, San Antonio, Texas, USA, 24–27 September. DOI: 10.2118/102542-MS.

Mattax, C.C. and Kyte, J.R. 1962. Imbibition Oil Recovery From Fractured, Water-Drive Reservoir. *SPE J.* 2 (2): 177–184; *Trans.*, AIME, **225**. SPE-187-PA. DOI: 10.2118/187-PA.

Ramirez, B., Kazemi, H., Al-Kobaisi, M., Ozkan, E., and Atan, S. 2007. A Critical Review for Proper Use of Water/Oil/Gas Transfer Functions in Dual-Porosity Naturally Fractured Reservoirs: Part I. *SPE Res Eval & Eng* **12** (2): 200–209. SPE-109821-PA. DOI: 10.2118/109821-PA.

Rangel-German, E.R. and Kovscek, A.R. 2003. Time-Dependent Matrix-Fracture Shape Factors for Partially and Completely Immersed Fractures. Paper SPE 84411 presented at the SPE Annual Technical Conference and Exhibition, Denver, 5–8 October. DOI: 10.2118/84411-MS.

Saidi, A.M. 1983. Simulation of Naturally Fractured Reservoirs. Paper SPE 12270 presented at the SPE Reservoir Simulation Symposium, San Francisco, 15–18 November. DOI: 10.2118/12270-MS.

Shinta, A.A. and Kazemi, H. 1993. Tracer Transport in Characterization of Dual-Porosity Reservoirs. Paper SPE 26636 presented at the SPE Annual Technical Conference and Exhibition, Houston, 3–6 October. DOI: 10.2118/26636-MS.

Sonier, F., Souillard, P., and Blaskovich, F.T. 1988. Numerical Simulation of Naturally Fractured Reservoirs. *SPE Res Eng* **3** (4): 1114–1122; *Trans.*, AIME, **285**. SPE-15627-PA. DOI: 10.2118/15627-PA.

Stoll, W.M., Hofman, J.P., Ligtheim, D.J., Faber, M.J., and van den Hoek, P.J. 2008. Toward Field-Scale Wettability Modification—The Limitation of Diffusive Transport. *SPE Res Eval & Eng* **11** (3): 633–640. SPE-107095-PA. DOI: 10.2118/107095-PA.

Uleberg, K. and Kleppe, J. 1996. Dual porosity, dual permeability formulation for fractured reservoir simulation. Presented at the Norwegian University of Science and Technology (NTNU), Trondheim RUTH Seminar, Stavanger.

Warren, J.E. and Root, P.J. 1963. The Behavior of Naturally Fractured Reservoirs. *SPE J.* 3 (3): 245–255; *Trans.*, AIME, **228**. SPE-426-PA. DOI: 10.2118/426-PA.

Yamamoto, R.H., Padgett, J.B., Ford, W.T., and Boubeguir, A. 1971. Compositional Reservoir Simulation for Fissured Systems—The Single-Block Model. *SPE J.* **11** (2): 113–128. SPE-2666-PA. DOI: 10.2118/2666-PA.

Zhang, X., Morrow, N.R., and Ma, S. 1996. Experimental Verification of a Modified Scaling Group for Spontaneous Imbibition. *SPE Res Eng* **11** (4): 280–285. SPE-30762-PA. DOI: 10.2118/30762-PA.

## Appendix A—Effect of High-Velocity Gas or Water Flow in Fracture on Transfer-Function Calculations

The transfer functions presented in Eqs. 2 and Eq. 14 were based on gravity-dominated flow in which the water and/or gas gradient is static in the fracture adjacent to a matrix block. This is consistent with field applications in which gas injection into the top of a naturally fractured reservoir is used to cause gravity drainage from the matrix. In such applications, the gas/oil-contact frontal velocity is kept on the order of a few feet per year, which makes the gas-flow-potential gradient essentially the same as the static gas gradient. Similar effects are in place when water encroaches into the fractures from an aquifer or from water injection into the aquifer or the lower part of the reservoir. The following sections give an example for both gas/oil and water/oil flow respectively.

### Gas/Oil Flow

For the gas/oil simulation, we injected gas at the top of the fracture and produced gas from the bottom of the fracture. In this case the gas-phase potential gradient in the fracture is given by:

$$(\Phi_{f2} - \Phi_{f1})/L_z = -a_g, \dots \dots \dots (A-1)$$

where  $\Phi_{f1}$  is the flow potential at Point 1 at the top of the fracture,  $\Phi_{f2}$  is the flow potential at Point 2 at the bottom of the fracture,  $L_z$  is the fracture height, and  $a_g$  is a positive number which makes the gas-flow potential negative for downward flow of gas (as it should be). Eq. A-1 can be written as follows:

$$\frac{(p_{f2} - \gamma_g D_2) - (p_{f1} - \gamma_g D_1)}{L_z} = -a_g, \dots \dots \dots (A-2)$$

Rearranging,

$$\frac{(p_{f2} - p_{f1}) - \gamma_g(D_2 - D_1)}{L_z} = -a_g, \dots \dots \dots (A-3)$$

Because  $D_2 - D_1$  is equal to  $L_z$ , Eq. A-3 becomes

$$\frac{p_{f2} - p_{f1}}{L_z} = \gamma_g - a_g, \dots \dots \dots (A-4)$$

Eq. A-4 indicates that the dynamic gas gradient in the fracture is smaller than the static gas gradient by  $a_g$ . Thus, to account for the gas-flow gradient in high-flow-rate experiments, we could replace  $\gamma_g$  in the gas/oil transfer function, Eq. A-5, by  $\gamma_g - a_g$ :

$$\tau_g = \sigma k_m \left\{ \frac{\lambda_{gf} \lambda_{om}}{\lambda_{gf} + \lambda_{om}} \left[ \frac{-(P_{cgom}^n - P_{cgo}^n)}{+ \frac{\sigma_z}{\sigma} (\gamma_o - \gamma_g) (h_{gf} - h_{gm})} \right] \right\} \dots \dots (A-5)$$

### Example.

- $q_g = 20.0$  Mscf/d
- $B_g = 0.0045$  res ft<sup>3</sup>/scf
- $\mu_g = 0.024$  cp
- $w_f = 0.1$  ft
- $L_x = 20$  ft
- $L_z = 20$  ft
- $k_f = 10,000$  md
- $k_{r,gf} = 0.99$
- $\rho_g = 11.5$  lbm/res ft<sup>3</sup>

### Calculations:

$\gamma_g = 11.5 / 144 = 0.0749$  psi/ft,  
 $q_g = -0.006328 \frac{k k_{r,gf}}{\mu_g B_g} (w_f L_x) \frac{\Phi_{f2} - \Phi_{f1}}{L_z}$ ,  
 and  
 $20,000 = -0.006328 \frac{(10,000)(0.99)}{(0.024)(0.0045)} (0.1) (20) \frac{\Phi_{f2} - \Phi_{f1}}{L_z}$ .  
 Thus,  $\frac{\Phi_{f2} - \Phi_{f1}}{L_z} = -0.0172$  psi/ft.  
 From Eq. A-1,  $a_g = 0.0172$  psi/ft.  
 From Eq. A-4, the effective gas gradient (could be used in the gas/oil transfer function) is

$$\gamma_{g,eff} = \gamma_g - a_g = 0.0749 - 0.0172 = 0.0577 \text{ psi/ft.}$$

The above effective gas gradient makes gas appear to be lighter than the gas at static conditions.

### Water/Oil Flow

For water/oil flow, water enters from the bottom of the fracture (Point 1) and exits the top of the fracture (Point 2). The water-phase potential gradient in the fracture is given by

$$(\Phi_{f2} - \Phi_{f1})/L_z = -a_w, \dots \dots \dots (A-6)$$

where  $\Phi_{f1}$  is the flow potential at Point 1 at the bottom of the fracture,  $\Phi_{f2}$  is the flow potential at Point 2 at the top of the fracture,  $L_z$  is the fracture height, and  $a_w$  is a positive number that makes the water-flow potential negative for upward flow of water (as it should be). Eq. A-6 can be written as

$$\frac{(p_{f2} - \gamma_w D_2) - (p_{f1} - \gamma_w D_1)}{L_z} = -a_w, \dots \dots \dots (A-7)$$

or as

$$\frac{(p_{f2} - p_{f1}) - \gamma_w(D_2 - D_1)}{L_z} = -a_w, \dots \dots \dots (A-8)$$

Because  $D_2 - D_1$  is equal to  $(-L_z)$ , Eq. A-8 becomes

$$\frac{p_{f2} - p_{f1}}{L_z} = -\gamma_w - a_g = -(\gamma_w + a_w), \dots \dots \dots (A-9)$$

Eq. A-9 indicates that the dynamic water gradient in the fracture is larger than the static water gradient by  $a_w$ . Thus, to account for the water-flow gradient, we could replace  $\gamma_w$  in the water/oil transfer function, Eq. A-10, by  $\gamma_w + a_w$ .

$$\tau_w = \sigma k_m \left\{ \frac{\lambda_{wf} \lambda_{om}}{\lambda_{wf} + \lambda_{om}} \left[ \frac{(P_{cwom}^n - P_{cwof}^n)}{\sigma} (\gamma_w - \gamma_o) (h_{wf} - h_{wm}) \right] \right\} \dots \dots \dots (A-10)$$

**Example.**

- $q_w = 0.70$  STB/D
- $B_w = 1.0$  RB/STB
- $\mu_w = 0.70$  cp
- $w_f = 0.1$  ft
- $L_x = 20$  ft
- $L_z = 20$  ft
- $k_f = 10,000$  md
- $k_r w_f = 0.99$
- $\rho_w = 62.4$  lbm/res ft<sup>3</sup>
- $\gamma_w = 62.4/144 = 0.433$  psi/ft

Calculations:

$$\gamma_w = 0.433 \text{ psi/ft,}$$

$$q_w = -0.006328 \frac{k k_r w_f}{\mu_w B_w} (w_f L_x) \frac{\Phi_{f2} - \Phi_{f1}}{L_z},$$

$$0.70 \times 5.6146 = -0.006328 \frac{(10,000)(0.99)}{(0.7)(1)} (0.1)(20) \frac{\Phi_{f2} - \Phi_{f1}}{L_z}.$$

Thus,  $\frac{\Phi_{f2} - \Phi_{f1}}{L_z} = -0.022$  psi/ft.

From Eq. A-6,  $a_w = 0.022$  psi/ft.

From Eq. A-4, the effective water gradient (could be used in the water/oil transfer function) is

$$\gamma_{w,eff} = \gamma_w + a_w = 0.4333 + 0.022 = 0.4553 \text{ psi/ft.}$$

The above effective water gradient makes water seem to be heavier than water at the static water gradient for a water rate of 0.70 RB/D. When we used a water rate of 20 RB/D as an example, the effective water gradient was  $0.4333 + 0.6286 = 1.0619$  psi/ft. Thus, gravity had a much greater influence on oil recovery from the matrix, but such high rates do not occur in practice. Nonetheless, if one uses such high rates in simulation, the results can be corrected to field situations.

**SI Metric Conversion Factors**

cp × 1.0*	E - 03 = Pa·s
ft × 3.048*	E - 01 = m
ft <sup>2</sup> × 9.290 304*	E - 02 = m <sup>2</sup>
ft <sup>3</sup> × 2.831 685	E - 02 = m <sup>3</sup>
lbm × 4.535 924	E - 01 = kg
psi × 6.894 757	E + 00 = kPa

\*Conversion factor is exact.

**Mohammed Al-Kobaisi** is a reservoir engineer with Abu Dhabi National Oil Corporation (ADNOC). He holds BS and MS degrees in petroleum engineering from Colorado School of Mines, where he is currently a PhD candidate. **Hossein Kazemi** is the Chesebro Distinguished Professor of Petroleum Engineering at Colorado School of Mines and Codirector of MCERS. He holds BS and PhD degrees in petroleum engineering from the U. of Texas at Austin in (1961 and 1963, respectively). Kazemi is a member of the National Academy of Engineering, a distinguished and an honorary member of SPE. He has published numerous technical papers and has served as distinguished author and speaker for the SPE. Kazemi retired from Marathon Oil Corporation in 2001 after serving as research scientist, senior technical consultant, director of production research, manager of reservoir technology, and executive technical fellow at Marathon Petroleum Technology Center in Littleton, Colorado. At Colorado School of Mines, he has taught graduate courses in petroleum engineering and supervised graduate research in reservoir modeling, well testing, and improved oil and gas recovery. **Benjamin Ramirez** is a reservoir engineer with Marathon Oil Corporation. He holds a BS in mechanical engineering from U. de los Andes and an MS in petroleum engineering from the Colorado School of Mines. **Erdal Ozkan** is a professor of petroleum engineering and codirector of MCERS at Colorado School of Mines. He holds BS and MS degrees from Istanbul Technical University and a PhD degree from the University of Tulsa, all in petroleum engineering. Since 1989, Ozkan has taught at Istanbul Technical University and Colorado School of Mines. His main research interests are pressure-transient analysis, modeling fluid flow in porous media, horizontal and multilateral well technology, and unconventional reservoirs. Ozkan served as the Executive Editor of *SPE Res Eval & Eng* and as the Editor in Chief of Elsevier *B.V. J. of Petroleum Science and Engineering*. He is the recipient of the 2007 SPE Formation Evaluation Award. **Safian Atan** is a reservoir engineer with Marathon Oil Corporation. He holds BS, ME, and PhD degrees in petroleum engineering from Colorado School of Mines.